Editors' Suggestion

Approximate Normalizations for Approximate Density Functionals

Adam Clay,[1] Kiril Datchev,[1] Wenlan Miao,[2] Adam Wasserman,[2,3] Kimberly J. Daas,[4] and Kieron Burke[4,5]
[1]*Department of Mathematics, Purdue University, West Lafayette, Indiana 47907, USA*
[2]*Department of Physics and Astronomy, Purdue University, West Lafayette, Indiana 47907, USA*
[3]*Department of Chemistry, Purdue University, West Lafayette, Indiana 47907, USA*
[4]*Department of Chemistry, University of California, Irvine, California 92697, USA*
[5]*Department of Physics and Astronomy, University of California, Irvine, California 92697, USA*

(Received 23 April 2025; accepted 17 December 2025; published 27 February 2026)

It seems self-evident that a density functional calculation should be normalized to the number of electrons in the system. We present multiple examples where the accuracy of the approximate energy is improved (sometimes greatly) by violating this basic principle. In one dimension, we explicitly derive the appropriate correction to the normalization. Beyond one dimension, Weyl asymptotics for energy levels yield these corrections for any cavity. We include examples with Coulomb potentials and the exchange energy of atoms to illustrate relevance to realistic calculations.

DOI: 10.1103/nc2l-yynf

It is a truth universally acknowledged, that any density functional calculation should yield a density that integrates to the number of electrons in the system. No matter how little is known about the functionals involved, this truth is so well fixed in the minds of practitioners that the normalization step passes almost unnoticed [1].

Sophisticated approximations to the exchange-correlation functional of Kohn-Sham density functional theory (DFT) [2,3], together with improved algorithms and powerful computers, allow for efficient and accurate calculations on systems with thousands of atoms [4]. With advances in quantum embedding methods [5] and orbital-free DFT [6], even millions of atoms can be treated [7], with applications ranging from molecular biology [8] to drug design [9] and materials engineering [10]. But in the 60 years since the foundational papers, it has never been questioned that, even when minimizing an approximate energy functional, the best normalization constraint is to require that $\int d\mathbf{r}\, n(\mathbf{r}) = N$, i.e., the density integrates to the number of electrons in the system. However, motivated by recent advances in the semiclassical study of DFT [11,12], we show here that an approximate normalization $\int d\mathbf{r}\, n(\mathbf{r}) = \widetilde{N} = N + \Delta N$, derived from asymptotic considerations, yields much better energetics than the usual norm. Remarkably, changing just this normalization and nothing else often yields better results than the same functional evaluated on the exact density (the basic idea behind density-corrected DFT improvements [13–16]). This also represents the generalization of many semiclassical DFT results beyond one dimension [12,17–20].

We start with a simple example: N noninteracting, spinless electrons in one dimension [21]. The local density approximation for such problems is the Thomas-Fermi (TF) approximation for the kinetic energy [22,23], here $\pi^2 \int dx n(x)^3/6$ (using Hartree atomic units). For the simplest case, the infamous particle(s) in a box, with the potential inside the box $v(x) = 0$ and box length $L = 1$, Fig. 1 compares three approximations for the energy $E(N)$. The first is the standard DFT treatment, where $n(x)$ is found by minimizing the functional, so $n(x) = N$. This energy is

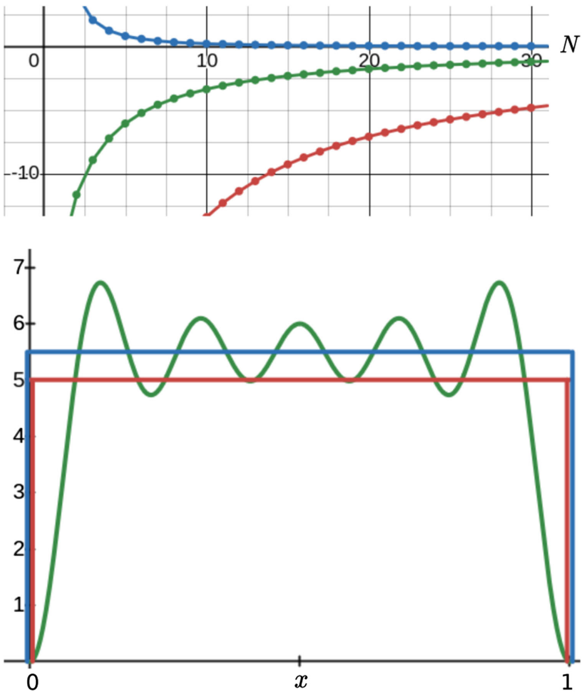

FIG. 1. Bottom: red is the TF density, green the exact density, and blue the normalization-corrected density for $N = 5$. Top: percent errors for the TF energy evaluated on each density (see Table S1 in [25]).

denoted $\widetilde{E}(N)$ (tilde signifies an approximation) and shown in red in the top panel, with its density in the bottom. The green is the TF functional evaluated on the exact density, with its energy denoted by $\widetilde{E}_{\rm d}(N)$ [24]. The blue is normalization-corrected TF (ncTF),

$$\widetilde{E}_{\rm nc}(N) = \widetilde{E}(\widetilde{N}), \qquad \widetilde{N} = N + \Delta N, \tag{1}$$

where $\widetilde{N}$ denotes an approximate normalization and where $\Delta N = 1/2$, outperforming $\widetilde{E}(N)$ and $\widetilde{E}_{\rm d}(N)$ in all cases. Energy expressions can be found in Sec. S1 of Supplemental Material [25]. The normalization correction makes the approximate density closer to the true density far from the walls, an idea that dates back to Scott [26].

In this first example, the correction ΔN can be derived from the explicit formula for the density $n(x) = \widetilde{N} - r(x)$, where $r(x) = \sin(2\widetilde{N}\pi x)/2\sin(\pi x)$ is a lower order term on average, away from the walls. Ignoring the density oscillations yields a better energy than accounting for them and has the advantage of staying within the family of densities belonging to the TF functional. In mathematical terms, the TF densities of differing $\widetilde{N}$ form a "foliation" of the graph space [27]. For a box or cavity, TF densities are constants and our correction yields the constant which best approximates the bulk, at the expense of the edge. Our approximate constraint beats the exact constraint and even beats using the exact density.

This Letter presents a proof of principle for our method, focusing on the noninteracting TF kinetic energy functional [22,23], which was first mathematically analyzed in [28,29]. We first derive and generalize the one-dimensional (1D) example above, using WKB theory [30]. We next explain how Weyl asymptotics for energy levels in cavities can be used to derive values of ΔN in higher dimensions, with various examples; for instance, Fig. 2 is the analog of the bottom panel of Fig. 1 for a 2D circular cavity (see also Ref. [31]). We also give several examples for specific simple potentials, ending with interacting systems and the exchange energy to connect to realistic DFT calculations.

Proof in one dimension—For the Hamiltonian $-(1/2)d^2/dx^2 + v(x)$, the TF and WKB approximations are essentially equivalent [33]. From WKB [Eq. (1.308) of [34]], under reasonable conditions on $v(x)$ [35], we have an implicit formula for individual energy levels

$$\int_{-\infty}^{\infty} \frac{dx}{\pi} p(\mathcal{E}, x) = \lambda(j) \coloneqq j - \nu + r(j), \tag{2}$$

where $p(\mathcal{E}, x) = \sqrt{2[\mathcal{E} - v(x)]_+}$ is the classical momentum, j is a positive integer, ν is the Maslov index [36] (0 if there are only hard walls and increases by $1/4$ for each classical turning point), and $r(j)$ is a remainder, which vanishes at least as fast as j^{-1}. The exact levels are

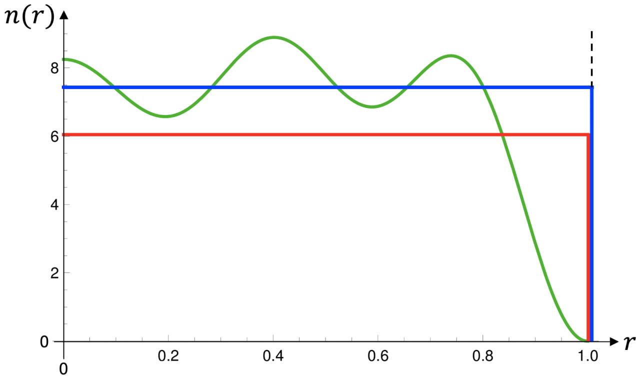

FIG. 2. Densities for 19 electrons (11 filled shells) in a circular cavity of radius 1. Green is the exact density, red is TF, and blue is ncTF (Sec. S7 of [25], which includes [32]). An analogous phenomenon, also derived from Weyl asymptotics, is observed in Fig. 2 of [31].

$$\mathcal{E}_j = \mathcal{E}\big(\lambda(j)\big) = \mathcal{E}\big(j - \nu + r(j)\big),$$

where $\mathcal{E}(\lambda)$ solves Eq. (2). Summing over N levels yields, for the dominant behavior as $N \to \infty$,

$$E(N) = \sum_{j=1}^{N} \mathcal{E}_j \sim \int_0^N d\lambda\, \mathcal{E}(\lambda). \tag{3}$$

By changing variables $\lambda \to \mathcal{E}$, differentiating (2), and swapping the order of integration, [33] showed that $\int_0^N d\lambda \mathcal{E}(\lambda) = \widetilde{E}(N)$, precisely [37].

An exact version of (3), similar to [38], is

$$E(N) = \int_{1/2}^{N+1/2} d\alpha \Big(\mathcal{E}\big(\lambda(\alpha)\big) + s(\alpha)\frac{d}{d\alpha}\mathcal{E}\big(\lambda(\alpha)\big)\Big), \tag{4}$$

where $s(\lambda) = \lambda - \lfloor \lambda \rfloor - 1/2$ is a sawtooth function, and we have extended $\lambda(\alpha)$ from (2) smoothly to noninteger α. To check (4), integrate by parts in the second term and simplify. Assuming certain derivatives of $\mathcal{E}(\lambda)$ and $r(\alpha)$ are well behaved, from (4) the leading correction to (3) is

$$E(N) \sim \int_0^{N+1/2-\nu} d\lambda\, \mathcal{E}(\lambda) = \widetilde{E}(N + 1/2 - \nu). \tag{5}$$

This yields $\Delta N = 1/2 - \nu$, so $\Delta N = 1/2$ in the two-wall case of the Introduction (first row of Table III) and $\Delta N = 1/4$ in the one-wall case (second and third rows of Table III). This completes the derivation of ΔN for any potential in 1D, with any nonperiodic boundary condition. For a harmonic oscillator, $\mathcal{E}(\lambda) = \omega\lambda$, $\nu = 1/2$, for a particle in a box, $\mathcal{E}(\lambda) = \pi^2\lambda^2/2L^2$, $\nu = 0$, and for a linear half well $\mathcal{E}(\lambda) = (3\pi\lambda/2)^{2/3}$, $\nu = 1/4$.

Weyl asymptotics—In higher dimensions, Weyl asymptotics [39,40] provide precise information about energy levels for many Hamiltonians, including general classes of

TABLE I. Exact and approximate energies for a 3D box with incommensurate edges $1 \times \sqrt{2} \times \pi$. See Fig. 3 and Supplemental Material Fig. S3 [25].

N	$E(N)$	$\widetilde{E}(N)$	$\widetilde{E}_{\mathrm{d}}(N)$	$\widetilde{E}_{\mathrm{nc}}(N) = \widetilde{E}(\widetilde{N})$
1	7.90	1.69(−79%)	3.61(−54%)	5.38(−32%)
10	161	78.3(−51%)	120(−26%)	148(−8%)
100	5141	3633(−29%)	4490(−13%)	5039(−2%)
1000	198 838	168 647(−15%)	187 810(−6%)	197 873(−0.5%)

potentials and cavities [41]. To derive a good ΔN from such asymptotics is simple. For N noninteracting, spinless electrons in a d-dimensional cavity, Weyl asymptotics state that

$$E(N) = C_1 N^{1+2/d} + C_2 N^{1+1/d} + \cdots, \tag{6}$$

where C_1 and C_2 depend on the geometry of the cavity in a simple, explicit way [Eq. (6) of [42]]; see also Ref. [31]. Related asymptotics hold for other Hamiltonians [41,43]. The TF approximation yields precisely the first term only, and we choose $\widetilde{N}$ to recover the second as $N \to \infty$. Thus, $\widetilde{E}(N)$ corresponds to a one-term Weyl asymptotic and $\widetilde{E}_{\mathrm{nc}}(N) = \widetilde{E}(\widetilde{N})$ to a two-term Weyl asymptotic. Table I and Fig. 3 show the accuracy of $\widetilde{E}_{\mathrm{nc}}(N)$ for a 3D box.

Weyl asymptotics were conjectured over a century ago in [40] and proved in [44,45]. They apply to problems in acoustics and blackbody radiation and are important throughout mathematics and physics [43]. The relevant quantities are averaged versions of the traditional asymptotics, which have been recently proven for very general cavities [46–49].

Generality—Table III presents further and richer examples of our method. In all cases, we find

$$\widetilde{E}(N) = AN^p, \qquad \Delta N = BN^q. \tag{7}$$

A key feature is that the formula for the correction power q, unlike those for p, A, or B, is universal. Moreover, the sign of B follows that of divergences in the potential, intuitively matching the error in the TF density in the interior. Figure 4 shows the significance of the normalization correction across cavities of different shapes. B increases with aspect ratio, so TF correspondingly loses accuracy, while ncTF remains accurate even for very elongated boxes. The formula $\Delta N = (|\partial\Omega|/3\sqrt{|\Omega|\pi})N^{1/2}$ works for 2D cavities of any shape, with $|\Omega|$ being the area of the cavity and $|\partial\Omega|$ the perimeter. Table II lists results for a circular cavity, where $\Delta N = (2/3)N^{1/2}$.

Generally, the more accurate an approximate energy functional is, the smaller ΔN is, but a good choice of ΔN improves energies (ΔN vanishes for the 1D harmonic oscillator because of perfect cancellation of errors in TF). Typically ΔN is small when the potential is smooth. For the two-dimensional isotropic harmonic oscillator $\Delta N = 1/24$ when all shells are filled, while the exact energy is

$$E(N) = \frac{\omega}{3} N\sqrt{8N+1}. \tag{8}$$

Neither of these examples fit in Table III because, in both cases, the leading correction is zero.

We have given general formulas for ΔN in 1D, for any cavity in any dimension, and for specific cases. A more general formula for ΔN as a functional of the potential $v(\mathbf{r})$ would be very powerful and could come from a more general version of the Weyl asymptotics (6). Some relevant asymptotics have been computed for smooth potentials in [50,51], and the large body of work on the Scott correction, which corresponds to the Coulomb case, is discussed in [52]. It is natural to expect a formula involving a phase space integral, in the spirit of [33].

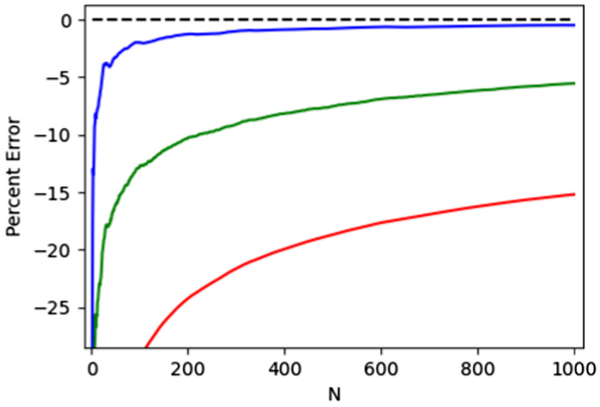

FIG. 3. Red is energy-minimized TF, green is TF on the exact density, and blue is normalization-corrected TF, for a $1\times\sqrt{2}\times\pi$ box.

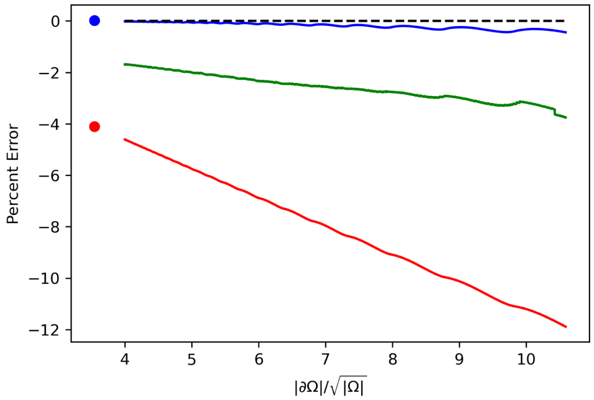

FIG. 4. Red is TF, green is TF on the exact density, and blue is ncTF, for a range of rectangular boxes (continuous) and for a circular cavity (discrete) at $N = 1000$. The dimensionless $|\partial\Omega|/\sqrt{|\Omega|}$ is proportional to B (Table III) and equals $2\sqrt{\pi}$ for a circle and 4 for a square (see Secs. S6 and S7 of [25]).

TABLE II. Exact and approximate energies for a circular cavity of radius 1. (Energy expressions in Sec. S7 of [25].).

N	$E(N)$	$\widetilde{E}(N)$	$\widetilde{E}_{\mathrm{nc}}(N) = \widetilde{E}(\widetilde{N})$
19	487	361 (−26%)	480 (−2%)
30	1139	900 (−21.0%)	1132 (−0.6%)
100	11 408	10 000 (−12%)	11 378 (−0.3%)
1000	1 042 850	1 000 000 (−4%)	1 042 608 (−0.02%)

Interacting electrons—In practical applications of DFT, electrons are subject to Coulomb repulsion. In this many-body problem, there is a very specific semiclassical limit of all (nonrelativistic) matter, in which the one-body potential is scaled along with N. In the special case of neutral atoms, this corresponds to simply keeping $Z = N$, where Z is the number of protons in the nucleus.

Over many decades, the asymptotic expansion for neutral atoms was derived,

$$E(N) = -c_0 N^{7/3} + N^2/2 - c_2 N^{5/3} + \cdots,$$

where $c_0 = 0.769\,745\ldots$ and $c_2 = 0.269\,900\ldots$ [12,26,53] and orbitals are doubly occupied. Here, TF theory (including the Hartree approximation for the electron-electron repulsion) yields precisely the first term alone, while the second is the Scott correction [12,26,54]. Setting $\Delta N = -3(14c_0)^{-1}N^{2/3}$ recovers the Scott correction, yielding the results in Table IV. The asymptotic expansion of $\widetilde{E}_{\mathrm{nc}}$ yields a correction with $\widetilde{c}_2 = 5/(28c_0) = 0.232\ldots$, within 15% of the correct value.

The Bohr atom—We can relate the interacting case above back to our noninteracting examples. The Bohr atom [12,57–59] consists of noninteracting fermions (singly) occupying hydrogenic orbitals. If the first k shells are filled, $N = 1^2 + 2^2 + \cdots + k^2$, and $k(N)$ is the inverse function, then

$$E(N) = -\frac{Z^2}{2}k(N) = -\frac{Z^2}{2}\left((3N)^{1/3} - \frac{1}{2} + \cdots\right). \quad (9)$$

We consider two distinct expansions. In the first, $Z = 1$ and $N \gg 1$, as in all our noninteracting examples. In the second, $Z = N \gg 1$, as for interacting problems. In Fig. 5 (and Table S2 of [25]), both significantly improve over simple TF, but the latter is more accurate, even more so than the Scott correction itself.

Exchange correlation—The Kohn-Sham (KS) scheme approximates only a small portion of the energy, the exchange correlation (XC) energy. The simplest approximation is the local density approximation for exchange (LDAX) [60–62], which underestimates its magnitude [63]. It uses the exchange energy density of electrons in an infinite box, analogous to the TF calculation for Fig. 1. We take an optimistic leap and imagine that the same forms of Table III apply to LDAX and simply multiply the density by a factor $1 + \Delta N/N$, with $\Delta N = BN^{2/3}$. This yields the normalization-corrected value

$$E_{\mathrm{X}}^{\mathrm{LDA}}(\mathrm{NC}) = (1 + B/N^{1/3})^{4/3} E_{\mathrm{X}}^{\mathrm{LDA}}. \quad (10)$$

Choosing $B = 0.125$ by eye, we find the remarkable improvements shown in Table V for the noble gas atoms, mirroring those for the total energy. The work of [31] derives the exact same form for the exchange asymptotics in a 3D box, with $B \approx 0.47$ (see Sec. S9 of [25]), consistent

TABLE III. Constants in Eq. (7). The 1D results are from Eq. (5), and those for cavities from Weyl asymptotics are from Eq. (6). The quarter harmonic (Secs. S4 and S5 of [25]) and Coulomb [Eq. (9)] results come from explicit formulas for eigenvalues.

d	Example	Potential	p	A	B	q
1	Interval of length $\lvert\Omega\rvert$	0 on $(0, \lvert\Omega\rvert)$ and $+\infty$ elsewhere	3	$(\pi^2/6\lvert\Omega\rvert^2)$	$\frac{1}{2}$	$[(d-1)/d]$
1	Half harmonic oscillator of frequency ω	$\frac{1}{2}\omega x^2$ on $(0, \infty)$ and $+\infty$ elsewhere	2	ω	$\frac{1}{4}$	$[(d-1)/d]$
1	Half linear well of strength F	Fx on $(0, \infty)$ and $+\infty$ elsewhere	$\frac{5}{3}$	$[3(3\pi F)^{2/3}/10]$	$\frac{1}{4}$	$[(d-1)/d]$
2	Cavity of area $\lvert\Omega\rvert$ and perimeter $\lvert\partial\Omega\rvert$	0 on $\Omega \subset \mathbb{R}^2$ and $+\infty$ elsewhere	2	$(\pi/\lvert\Omega\rvert)$	$(\lvert\partial\Omega\rvert/3\sqrt{\lvert\Omega\rvert\pi})$	$[(d-1)/d]$
2	Quarter harmonic oscillator of frequency ω	$\frac{1}{2}\omega r^2$ on $(0, \infty) \times (0, \infty)$ and $+\infty$ elsewhere	$\frac{3}{2}$	$(4\sqrt{2}/3)\omega$	$(1/2\sqrt{2})$	$[(d-1)/d]$
3	Cavity of volume $\lvert\Omega\rvert$ and surface area $\lvert\partial\Omega\rvert$	0 on $\Omega \subset \mathbb{R}^3$ and $+\infty$ elsewhere	$\frac{5}{3}$	$[3(6\pi^2)^{\frac{2}{3}}/10\lvert\Omega\rvert^{\frac{2}{3}}]$	$[(36\pi)^{\frac{1}{3}}\lvert\partial\Omega\rvert/32\lvert\Omega\rvert^{\frac{2}{3}}]$	$[(d-1)/d]$
3	Int. Coulomb, $Z = N$	$-(Z/r)$ on $\mathbb{R}^3\backslash\{0\}$, $Z = N$	$\frac{7}{3}$	$-c_0$	$-(3/14c_0)$	$[(d-1)/d]$
3	Nonint. Coulomb, $Z = N$	$-(Z/r)$ on $\mathbb{R}^3\backslash\{0\}$, $Z = N$	$\frac{7}{3}$	$-(3^{\frac{1}{3}}/2)$	$-(3^{\frac{2}{3}}/14)$	$[(d-1)/d]$
3	Nonint. Coulomb, Z fixed	$-(Z/r)$ on $\mathbb{R}^3\backslash\{0\}$	$\frac{1}{3}$	$-(3^{\frac{1}{3}}/2)$	$-(3^{\frac{2}{3}}/2)$	$[(d-1)/d]$

TABLE IV. Energies and percent errors for TF and ncTF for nonrelativistic noble gases. For $N \geq 10$, $E(N)$ is obtained by adding exchange-only energies from Table 4.6 of [55] and acGGA+ correlation corrections from Table I of [56] (correlation is unimportant, being less than 0.1 per electron).

			Percent errors	
Atom	N	$E(N)$	$\widetilde{E}(N)$	$\widetilde{E}_{\mathrm{nc}}(N)$
He	2	−2.904	−33	26
Ne	10	−128.9	−28	7
Ar	18	−527.6	−24	5
Kr	36	−2754	−19	2.8
Xe	54	−7235	−17	2.1
Rn	86	−21870	−15	1.5

TABLE V. Energies (percentage errors) for the noble gases with $\mathrm{EXX}(N)$ being the exact exchange energy, $E_{\mathrm{x}}^{\mathrm{LDA}}(N)$ the local density approximation exchange energy, $E_{\mathrm{x}}^{\mathrm{PBE}}(N)$ the Perdew-Burke-Ernzerhof (PBE) exchange energy, and $E_{\mathrm{nc}}^{\mathrm{LDA}}(N)$ the normalization-corrected LDA. The first three were obtained from [56].

Atom	N	$\lvert\mathrm{EXX}(N)\rvert$	$\lvert E_{\mathrm{x}}^{\mathrm{LDA}}(N)\rvert$	$\lvert E_{\mathrm{x}}^{\mathrm{PBE}}(N)\rvert$	$\lvert E_{\mathrm{nc}}^{\mathrm{LDA}}(N)\rvert$
He	2	1.026	0.862 (16%)	1.005 (2%)	0.978 (5%)
Ne	10	12.10	10.97 (9%)	12.03 (0.6%)	11.82 (2%)
Ar	18	30.18	27.81 (8%)	29.98 (0.64%)	29.59 (2%)
Kr	36	93.83	88.53 (6%)	93.38 (0.5%)	93.03 (0.9%)
Xe	54	179.1	170.5 (5%)	178.2 (0.5%)	178.1 (0.5%)
Rn	86	387.5	372.9 (4%)	385.9 (0.4%)	387.0 (0.1%)

with our guess. Their kinetic energy calculation agrees with our formulas and also yields a bulk density of $N + \Delta N$ per unit volume, just as in our examples.

Outlook—For a one-dimensional box, one can compute ΔN by eye from Fig. 1 by making the straight line of the approximate density go through the middle of the oscillations of the exact density. In less obvious cases, the practicality of normalization corrections will ultimately rely on more robust formulas for ΔN as a functional of the potential. The above derivations based on WKB and Weyl asymptotics are special cases of semiclassical asymptotics, which admit many general formulations [41,64–66]. Work deriving ΔN in a universal way from semiclassical trace formulas [50,51], building on the phase space point of view of [33,37], is ongoing. Our work emphasizes the need for results with open boundaries rather than cavities. Such results could lead to improvements in accuracy for orbital-free DFT calculations, which scale linearly in N, avoiding the cubic-in-N calculation of Kohn-Sham orbitals [6]. For applications to solids, these results should generalize to periodic boundary conditions. Thus, we make DFT accurate up to two orders instead of just the leading one in a way analogous to—but different from—corrections that were used to construct PBEsol [67] and SCAN [68].

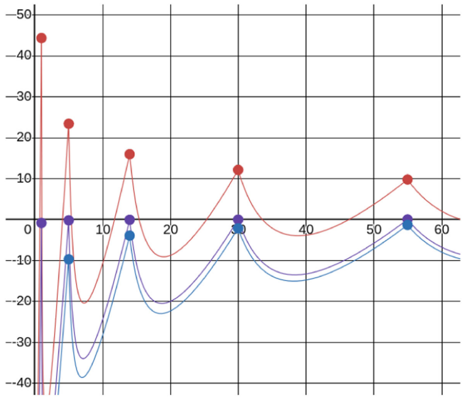

FIG. 5. Percent errors in Bohr atom energies for TF (red), ncTF with Z fixed (blue), and ncTF with $Z = N$ (purple). See Sec. S8 and Table S2 of [25].

The density with ΔN extra electrons is not the true density of the system; it is a device guaranteeing more accurate energetics by improving asymptotics. In principle, one could derive a correction to the TF density functional whose optimal density reproduces these energetics, by taking the functional derivative of the corrected energy with respect to the potential. In practice, this is a nontrivial derivation that likely requires some form of regularization in the vicinity of the boundaries.

In the future, there are many variations of our tricks that could be applied to the XC functional in a KS calculation, not just the one tried here. Important open problems include proving that our method is applicable to the XC energy, making it size extensive, and using it to guide the development of better functionals.

Our analysis is also relevant to improving "density-corrected DFT" (DC-DFT), a simple method that has become popular [13–15], where the self-consistent density is replaced by (a proxy for) the exact density. DC-DFT has proven successful in many applications, including ions in solution [69] and the phase diagram of water [70]. However, we have shown that a normalization correction of an approximate density can be more accurate than evaluation on the exact density. Our correction is also much easier to implement, not just in this example, but in every case we have considered.

Acknowledgments—The authors thank Thiago Carvalho Corso, Gero Friesecke, Hamid Hezari, and Antoine Prouff for helpful discussions. K. B. also thanks the Mathematisches Forschungsinstitut Oberwolfach for hospitality. K. B. was supported by the NSF Award No. CHE-2154371. K. J. D. thanks UCI's Chancellors Postdoctoral Fellowship Program and, in particular, Prof. Dr. Feizal Waffarn for his support as a sponsor. K. D. was supported by NSF Award No. DMS-1708511 and by a Simons Foundation Collaboration Grant for Mathematicians.

W. M. and A. W. were supported by NSF Award No. CHE-2306011.

Data availability—The data that support the findings of this article are openly available [71].

[1] J. Austen, *Pride and Prejudice* (T. Egerton, Whitehall, 1813).

[2] P. Hohenberg and W. Kohn, Inhomogeneous electron gas, Phys. Rev. B **136**, B864 (1964).

[3] W. Kohn and L. J. Sham, Self-consistent equations including exchange and correlation effects, Phys. Rev. **140**, A1133 (1965).

[4] M. Del Ben, O. Schütt, T. Wentz, P. Messmer, J. Hutter, and J. VandeVondele, Enabling simulation at the fifth rung of DFT: Large scale RPA calculations with excellent time to solution, Comput. Phys. Commun. **187**, 120 (2015).

[5] A. Wasserman and M. Pavanello, Quantum embedding electronic structure methods, Int. J. Quantum Chem. **120**, e26495 (2020).

[6] W. Mi, K. Luo, S. B. Trickey, and M. Pavanello, Orbital-free density functional theory: An attractive electronic structure method for large-scale first-principles simulations, Chem. Rev. **123**, 12039 (2023).

[7] W. Dawson, A. Degomme, M. Stella, T. Nakajima, L. E. Ratcliff, and L. Genovese, Density functional theory calculations of large systems: Interplay between fragments, observables, and computational complexity, WIREs Comput. Mol. Sci. **12**, e1574 (2022).

[8] D. J. Cole and N. D. M. Hine, Applications of large-scale density functional theory in biology, J. Phys. Condens. Matter **28**, 393001 (2016).

[9] O. C. Adekoya, G. J. Adekoya, E. R. Sadiku, Y. Hamam, and S. S. Ray, Application of DFT calculations in designing polymer-based drug delivery systems: An overview, Pharmaceutics **14**, 1972 (2022).

[10] M. K. Horton, S. Dwaraknath, and K. A. Persson, Promises and perils of computational materials databases, Nat. Comput. Sci. **1**, 3 (2021).

[11] M. V. Berry and K. Burke, Exact and approximate energy sums in potential wells, J. Phys. A **53**, 095203 (2020).

[12] P. Okun and K. Burke, Semiclassics: The hidden theory behind the success of DFT, in *Density Functionals for Many-Particle Systems* (World Scientific, Singapore, 2023), pp. 179–249.

[13] E. Sim, S. Song, S. Vuckovic, and K. Burke, Improving results by improving densities: Density-corrected density functional theory, J. Am. Chem. Soc. **144**, 6625 (2022).

[14] S. Vuckovic, S. Song, J. Kozlowski, E. Sim, and K. Burke, Density functional analysis: The theory of density-corrected DFT, J. Chem. Theory Comput. **15**, 6636 (2019).

[15] S. Song, S. Vuckovic, E. Sim, and K. Burke, Density-corrected DFT explained: Questions and answers, J. Chem. Theory Comput. **18**, 817 (2022).

[16] M.-C. Kim, E. Sim, and K. Burke, Understanding and reducing errors in density functional calculations, Phys. Rev. Lett. **111**, 073003 (2013).

[17] P. Okun, A. C. Cancio, and K. Burke, Orbital-free potential functionals with submillihartree errors for single-well slabs, Phys. Rev. B **109**, 195156 (2024).

[18] N. Argaman, J. Redd, A. C. Cancio, and K. Burke, Leading correction to the local density approximation for exchange in large-z atoms, Phys. Rev. Lett. **129**, 153001 (2022).

[19] P. Elliott, A. Cangi, S. Pittalis, E. K. U. Gross, and K. Burke, Almost exact exchange at almost no computational cost in electronic structure, Phys. Rev. A **92**, 022513 (2015).

[20] L. A. Constantin, E. Fabiano, S. Laricchia, and F. Della Sala, Semiclassical neutral atom as a reference system in density functional theory, Phys. Rev. Lett. **106**, 186406 (2011).

[21] R. F. Ribeiro, D. Lee, A. Cangi, P. Elliott, and K. Burke, Corrections to Thomas-Fermi densities at turning points and beyond, Phys. Rev. Lett. **114**, 050401 (2015).

[22] L. H. Thomas, The calculation of atomic fields, Math. Proc. Cambridge Philos. Soc. **23**, 542 (1927).

[23] E. Fermi, Un metodo statistico per la determinazione di alcune priopretà dell'atomo, Accademia Nazionale dei Lincei **6**, 602 (1927).

[24] P. Elliott, D. Lee, A. Cangi, and K. Burke, Semiclassical origins of density functionals, Phys. Rev. Lett. **100**, 256406 (2008).

[25] See Supplemental Material at http://link.aps.org/supplemental/10.1103/nc2l-yynf for additional details and data.

[26] J. Scott, LXXXII. The binding energy of the Thomas-Fermi atom, Lond. Edinb. Dubl. Phil. Mag. J. Sci. **43**, 859 (1952).

[27] A. Candel and L. Conlon, *Foliations, Volume 1*, Graduate Studies in Mathematics (American Mathematical Society, Providence, RI, 1999).

[28] E. H. Lieb and B. Simon, Thomas-Fermi theory revisited, Phys. Rev. Lett. **31**, 681 (1973).

[29] E. H. Lieb, Thomas-Fermi and related theories of atoms and molecules, Rev. Mod. Phys. **53**, 603 (1981).

[30] C. M. Bender and S. A. Orszag, *Advanced Mathematical Methods for Scientists and Engineers I* (Springer, New York, 1999).

[31] T. C. Corso and G. Friesecke, Next-order correction to the Dirac exchange energy of the free electron gas in the thermodynamic limit and generalized gradient approximations, J. Math. Phys. (N.Y.) **65**, 081902 (2024).

[32] G. N. Watson, *A Treatise on the Theory of Bessel Functions* (Cambridge University Press, Cambridge, England, 1944).

[33] N. H. March and J. S. Plaskett, The relation between the Wentzel-Kramers-Brillouin and the Thomas-Fermi approximations, Proc. R. Soc. A **235**, 419 (1956).

[34] H. Friedrich, *Theoretical Atomic Physics* (Springer International Publishing, New York, 2017), 10.1007/978-3-319-47769-5.

[35] E. C. Titchmarsh, On the asymptotic distribution of eigenvalues, Q. J. Mech. Appl. Math. **5**, 228 (1954).

[36] V. P. Maslov and M. V. Fedoriuk, *Semi-Classical Approximation in Quantum Mechanics*, 1981st ed., Mathematical Physics and Applied Mathematics (Kluwer Academic, Dordrecht, Netherlands, 1981).

[37] A. Cangi, D. Lee, P. Elliott, and K. Burke, Leading corrections to local approximations, Phys. Rev. B **81**, 235128 (2010).

[38] K. Burke, Deriving approximate functionals with asymptotics, Faraday Discuss. **224**, 98 (2020).

[39] H. Weyl, Ueber die asymptotische verteilung der eigenwerte, Gött. Nachr. Math. Phys. Klass. **1911**, 110 (1911).

[40] H. Weyl, Über die randwertaufgabe der strahlungstheorie und asymptotische spektralgesetze, crll **1913**, 177 (1913).

[41] V. Ivrii, 100 years of Weyl's law, Bull. Math. Sci. **6**, 379 (2016).

[42] E. M. Harrell II, L. Provenzano, and J. Stubbe, Complementary asymptotically sharp estimates for eigenvalue means of Laplacians, Int. Math. Res. Not. **2021**, 8405 (2019).

[43] W. Arendt, R. Nittka, W. Peter, and F. Steiner, Weyl's Law: Spectral Properties of the Laplacian in Mathematics and Physics, in *Mathematical Analysis of Evolution, Information, and Complexity*, edited by W. Arendt and W. P. Schleich (2009), 10.1002/9783527628025.ch1.

[44] J. J. Duistermaat and V. W. Guillemin, The spectrum of positive elliptic operators and periodic bicharacteristics, Inventiones Mathematicae **29**, 39 (1975).

[45] V. Y. Ivrii, Second term of the spectral asymptotic expansion of the laplace—Beltrami operator on manifolds with boundary, Funct. Anal. Appl. **14**, 98 (1980).

[46] R. L. Frank and L. Geisinger, Two-term spectral asymptotics for the Dirichlet Laplacian on a bounded domain, in *Mathematical Results in Quantum Physics* (World Scientific, Singapore, 2011).

[47] R. L. Frank and L. Geisinger, Semi-classical analysis of the laplace operator with robin boundary conditions, Bull. Math. Sci. **2**, 281 (2012).

[48] R. L. Frank and S. Larson, Two-term spectral asymptotics for the Dirichlet Laplacian in a Lipschitz domain, J. Reine Angew. Math. (Crelles J.) **2020**, 195 (2019).

[49] R. L. Frank and S. Larson, Riesz means asymptotics for Dirichlet and Neumann Laplacians on Lipschitz domains, Inventiones Mathematicae **241**, 999 (2025).

[50] B. Helffer and D. Robert, Riesz means of bound states and semiclassical limit connected with a Lieb–Thirring's conjecture, Asymptotic Analysis **3**, 91 (1990).

[51] V. Guillemin and Z. Wang, Semiclassical spectral invariants for Schrödinger operators, J. Diff. Geom. **91**, 103 (2012).

[52] R. L. Frank, K. Merz, and H. Siedentop, The Scott conjecture for large Coulomb systems: A review, Lett. Math. Phys. **113**, 11 (2023).

[53] J. Schwinger, Thomas-Fermi model: The second correction, Phys. Rev. A **24**, 2353 (1981).

[54] J. Schwinger, Thomas-Fermi model: The leading correction, Phys. Rev. A **22**, 1827 (1980).

[55] R. M. D. Eberhard Engel, *Theoretical, Mathematical & Computational Physics* (Springer-Verlag, Berlin, Heidelberg, 2011).

[56] A. Cancio, G. P. Chen, B. T. Krull, and K. Burke, Fitting a round peg into a round hole: Asymptotically correcting the generalized gradient approximation for correlation, J. Chem. Phys. **149**, 084116 (2018).

[57] O. J. Heilmann and E. H. Lieb, Electron density near the nucleus of a large atom, Phys. Rev. A **52**, 3628 (1995).

[58] B.-G. Englert, *Semiclassical Theory of Atoms* (Springer, Berlin, Heidelberg, 1988), 10.1007/3-540-19204-2.

[59] K. Burke, A. Cancio, T. Gould, and S. Pittalis, Locality of correlation in density functional theory, J. Chem. Phys. **145**, 054112 (2016).

[60] P. A. M. Dirac, Note on exchange phenomena in the Thomas atom, Math. Proc. Cambridge Philos. Soc. **26**, 376 (1930).

[61] F. Bloch, Bemerkung zur elektronentheorie des ferromagnetismus und der elektrischen leitfähigkeit, Z. Phys. **57**, 545 (1929).

[62] J. C. Slater, A simplification of the Hartree-Fock method, Phys. Rev. **81**, 385 (1951).

[63] H. Eschrig, *The Fundamentals of Density Functional Theory*, Teubner Texte Zur Physik (Vieweg+Teubner Verlag, Wiesbaden, Germany, 1996).

[64] M. Dimassi and J. Sjöstrand, *Spectral Asymptotics in the Semi-Classical Limit* (Cambridge University Press, Cambridge, England, 1999).

[65] M. Zworski, *Semiclassical Analysis* (American Mathematical Society, Providence, 2012).

[66] V. Guillemin and S. Sternberg, *Semi-Classical Analysis* (International Press, Somerville, Massachusetts, USA, 2013).

[67] J. P. Perdew, A. Ruzsinszky, G. I. Csonka, O. A. Vydrov, G. E. Scuseria, L. A. Constantin, X. Zhou, and K. Burke, Restoring the density-gradient expansion for exchange in solids and surfaces, Phys. Rev. Lett. **100**, 136406 (2008).

[68] J. Sun, A. Ruzsinszky, and J. P. Perdew, Strongly constrained and appropriately normed semilocal density functional, Phys. Rev. Lett. **115**, 036402 (2015).

[69] M.-C. Kim, E. Sim, and K. Burke, Ions in solution: Density corrected density functional theory (DC-DFT), J. Chem. Phys. **140**, 18A528 (2014).

[70] S. Song, S. Vuckovic, Y. Kim, H. Yu, E. Sim, and K. Burke, Extending density functional theory with near chemical accuracy beyond pure water, Nat. Commun. **14**, 799 (2023).

[71] https://zenodo.org/records/18603914